npj | climate and atmospheric science

Article

Published in partnership with CECCR at King Abdulaziz University

https://doi.org/10.1038/s41612-025-01314-3

Logarithmic CO_2 warming reverses North Atlantic winter atmospheric circulation changes

Rei Chemke[1] ✉ & Ivan Mitevski[2]

The North Atlantic climate is strongly influenced by large-scale atmospheric circulation, including the storm track and jet stream, which shape regional precipitation, temperature, and wind patterns. Climate models project an intensification of the winter circulation through the 21st century, however, it remains unclear whether abrupt or non-monotonic changes might occur under ongoing warming. Here we show that under continued CO_2 emissions beyond 2100, the intensification reverses, with both the storm track and jet stream returning toward their 20th-century states. We attribute this reversal to the logarithmic relationship between CO_2 and temperature, which leads to a reduced meridional temperature gradient and weakened atmospheric circulation at high CO_2 concentrations. This behavior also alters regional climate patterns, reversing storm track-induced warming and wetting at higher mid-latitudes and cooling and drying at lower mid-latitudes over eastern North America and the North Atlantic. Our findings suggest that mitigation policies should account for the pace of continued emissions as well as the potential reversals in climate impacts.

The North Atlantic region hosts key components of the climate system, including oceanic, atmospheric, and cryospheric processes. Ocean circulation—particularly the Atlantic Meridional Overturning Circulation (AMOC)—plays a central role in transporting heat between low and high latitudes and is sensitive to changes in Greenland ice cover. Atmospheric features such as the North Atlantic storm track and jet stream[1–5], as well as sea surface temperature variability[6] (e.g., Atlantic multidecadal variability), strongly influence weather and climate on both sides of the Atlantic. Consequently, considerable efforts have been devoted to understanding how these interconnected systems respond to anthropogenic emissions.

In particular, climate model projections consistently show an intensification (mostly over the eastward flank) of the winter North Atlantic storm track and jet stream by the end of the 21st century[1,7–11]. The intensification of the flow was argued to be driven by ocean heat transport changes[12], e.g., AMOC weakening was found to be associated with the changing flow[8,13]. These large-scale atmospheric flows modulate regional weather and climate by transporting heat, moisture, and momentum, thereby influencing patterns of precipitation, temperature and winds, including extreme events. Strengthening of these flows is expected to have major consequences not only for the buoyancy- and wind-driven ocean circulations but also for land regions over eastern North America and western Europe[14,15].

While changes in North Atlantic atmospheric circulation during the 21st century have been widely studied (providing valuable insight into near-future climate risks), it remains unclear whether these trends will persist, accelerate, or undergo abrupt or non-monotonic changes under ongoing warming beyond 2100–a critical aspect for designing effective mitigation strategies. There is a high potential for abrupt and non-monotonic changes in the large-scale atmospheric flow due to similar projected changes in several thermodynamic variables[16]. Indeed, recent work—including idealized modeling experiments[17]—has identified non-monotonic behavior in the mid-latitude storm track in the Southern Hemisphere under sustained CO_2 forcing in the 22nd century[18], as well as in Northern Hemisphere stratospheric winds under idealized forcing[19]. Here, by extending the analysis on winter North Atlantic atmospheric circulation changes beyond the 21st century, we aim to identify potential reversals or abrupt changes in the atmospheric circulation, with implications for better constraining the timing and magnitude of climate-change mitigation and adaptation strategies.

Results

Projected circulation changes beyond 2100

To examine the response of the North Atlantic winter (December-February) atmospheric circulation to a continuous increase in greenhouse gases beyond 2100, we first analyze model simulations from phase 6 of the Coupled Model Intercomparison Program (CMIP6) integrated under the

[1]Department of Earth and Planetary Sciences, Weizmann Institute of Science, Rehovot, Israel. [2]Department of Geosciences, Princeton University, Princeton, NJ, USA. ✉e-mail: rei.chemke@weizmann.ac.il

long-term extension of the Shared Socioeconomic Pathways 5-8.5 (SSP5-8.5) between the 21st and 23rd centuries. Under this scenario, CO_2 is projected to continue increasing through the first half of the 23rd century, reaching levels that are ~7.7 times larger than the preindustrial values (black lines in Fig. 1). Consistent with previous studies, over the course of the 21st century and continuing through the first half of the 22nd century, the intensity of both the North Atlantic storm track (calculated using the eddy kinetic energy, EKE) and the jet stream (Methods) is projected to increase (red lines in Fig. 1); the North Atlantic region is defined between 90°W − 30°E and 40°N − 60°N, where most of the intensification occurs (Supplementary Fig. 1).

By the mid-22nd century (the 2140–2160 period), the storm track intensifies by ~14% (Fig. 1a) and the jet stream by ~7% (Fig. 1b), relative to the 00's values (the 1990–2010 period). Surprisingly, despite the continued increase in CO_2 concentrations, starting from the mid-22nd century the circulation not only stops increasing but even weakens and almost fully recovers. By the end of the 23rd century (the 2280–2299 period), the storm track yields an increase of only ~3% and the jet stream of only ~0.2%, relative to the 00's values. The small decrease in CO_2 concentrations at the end of the simulation (black lines) may play a minor role in the late-23rd century weakening, yet most of the weakening occurs while CO_2 is still increasing. Lastly, we note that the reversibility in the circulation intensity is a regional feature of the North Atlantic (Supplementary Fig. 1), and is not evident in changes in the position of the flow (Supplementary Fig. 2); the North Atlantic jet stream was found to considerably shift poleward mostly during summer and autumn[20,21].

Given the impact of the circulation, especially the storm track, on precipitation and temperature patterns, we next assess the changes in the eddy horizontal heat and moisture flux (Methods) (Fig. 2). First, by the mid-22nd century, the eddy moisture flux convergence increases over the higher mid-latitudes (green colors) while decreasing at the lower mid-latitudes (brown colors) (Fig. 2a). A similar pattern is evident in eddy heat flux convergence (Fig. 2c). Overall, the eddies act to warm and wet the higher mid-latitudes, while cooling and drying the lower mid-latitudes, mostly over the Atlantic and eastern North America. These changes are consistent with the intensification of the storm track (Fig. 1a), i.e., an intensification of the poleward eddy heat and moisture fluxes. Second, from the mid-22nd century through the end of the 23rd century, similar to the reversal of the EKE, the above patterns also reverse, exhibiting drying and cooling (i.e., divergence of the fluxes) in the higher mid-latitudes, and wetting and warming (i.e., convergence of the fluxes) in the lower mid-latitudes (Fig. 2b, d).

The physics underlying the reversibility of the circulation

We turn to elucidate the physical mechanism underlying the reversibility of the North Atlantic circulation. To this end, we make use of a set of CO_2 runs, which allow us to cleanly isolate the link between CO_2 increase and the non-monotonic circulation behavior. Specifically, we start by examining the response of the North Atlantic storm track to abrupt CO_2 increases, ranging from 2× to 8× the preindustrial values, simulated with the Community Earth System Model (CESM) ("Methods"). Despite the idealized and fixed forcing (rather than the transient forcing in the SSP5-8.5 scenario), the abrupt runs are able to capture the non-monotonic increase in storm track intensity with respect to CO_2 (Fig. 3a). Namely, while at relatively low CO_2 levels (up to 4× the preindustrial values) the storm track intensifies, at relatively high CO_2 levels (above 4× the preindustrial values) the storm track slightly decreases. Although the abrupt runs do not capture the full reversibility of the storm track as in the transient runs (Fig. 1), we show below that they capture the key mechanism underlying the circulation recovery. We thus next leverage the abrupt runs to isolate the source of the North Atlantic circulation behavior.

The changes in storm track intensity can be understood by examining the eddy growth rate[10,12,22–24] (a commonly used metric that encapsulates the extraction of potential energy from the mean flow to the eddies). We calculate the eddy growth rate by applying a linear normal mode instability analysis to the quasigeostrophic potential vorticity equations, using the vertical structure of the North Atlantic mean zonal wind (U), temperature (static stability, N) and tropopause height (H) ("Methods"). Despite its relative simplicity, the eddy growth rate adequately captures the non-monotonic behavior of the storm track (compare black lines in Fig. 3a, b), including the increase up to 4 × CO_2, and the lack of it at higher CO_2 levels. Decomposing the relative contribution of each mean field to the growth rate response to CO_2 ("Methods") reveals that changes in the zonal wind shear account for the growth rate non-monotonic behavior, i.e., the increase at low CO_2 levels that plateaus at high CO_2 levels (red line in Fig. 3b). In contrast, static stability and tropopause height have minor mitigating impacts (blue and green lines in Fig. 3b). We note that similar results are found in the extended SSP5-8.5 runs (Supplementary Fig. 3a).

To identify the source of the nonlinear zonal wind shear behavior, we next examine the atmospheric temperature response at low and high CO_2 levels, averaged zonally over the North Atlantic region (Fig. 4), since the wind shear is in balance with the meridional temperature gradient (thermal wind balance). First, the temperature changes at low CO_2 levels (between 1 × CO_2 and 3 × CO_2) exhibit the canonical atmospheric warming pattern of enhanced warming in the upper tropical troposphere and Arctic amplification (warming in the lower polar troposphere) (Fig. 4a). Consistent with previous work examining the North Atlantic storm track intensification over the 21st century[12], the enhanced warming of the lower latitudes throughout most of the troposphere, relative to the higher latitudes, increases the meridional temperature gradient (the jet stream), and thus the eddy growth rate and the storm track intensity (Fig. 3a). Examining the temperature response to the same increase in CO_2 concentrations only at higher CO_2 levels (between 4 × CO_2 and 6 × CO_2) reveals a different warming pattern. The enhanced warming of the lower latitudes, which still exists, considerably weakens, while the polar amplification, although being reduced, is still considerable throughout the troposphere (Fig. 4b). As a result, opposite to low CO_2 levels, this pattern acts to reduce the meridional temperature gradient, and thus the jet stream and the storm track intensity (Fig. 3a). The evolution of the meridional temperature gradient across the mid-latitudes, further confirms this non-monotonic behavior (Supplementary Fig. 3b). These results join previous work on the larger impact of upper level warming, relative to lower level warming, on the mid-latitude flow[20,25–27], and specifically on the tendency of upper tropical tropospheric

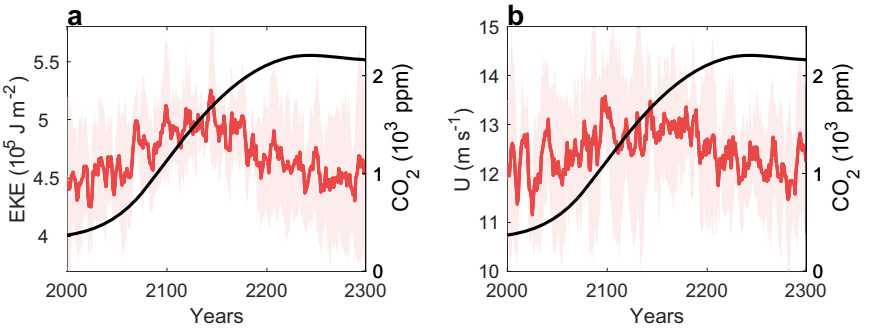

Fig. 1 | The reversibility of the North Atlantic circulation by 2300. The evolution of CO_2 (black lines) and the winter North Atlantic (**a**), eddy kinetic energy (EKE) and (**b**), jet stream (red) over the 2000–2300 period under the historical and SSP5-8.5 scenario. Red lines show the CMIP6 mean and shadings the standard deviation across the models, with a centered 5-year running mean for plotting purposes.

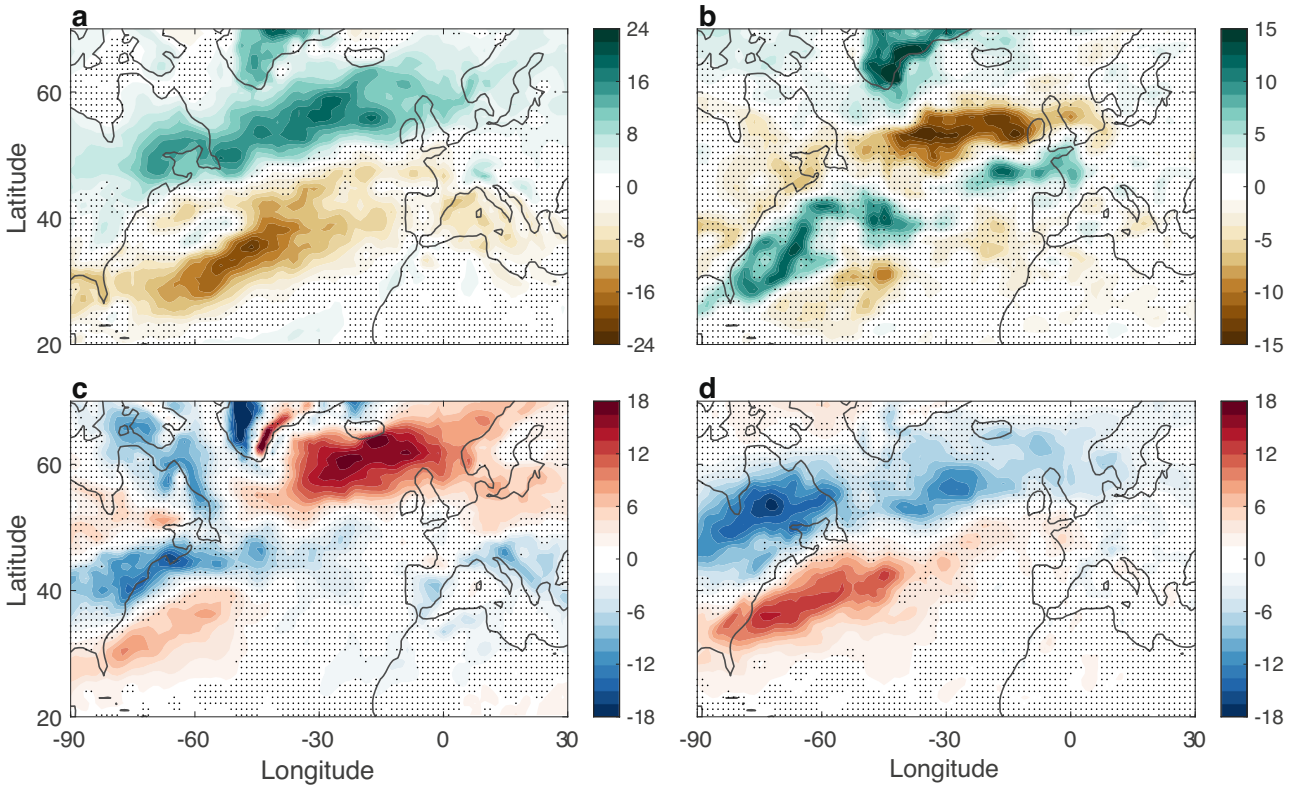

Fig. 2 | The impacts of the recovering North Atlantic storm track. The changes in the eddy flux convergence (W m^{-2}) of **a**, **b**, moisture and **c**, **d**, heat over the periods of intensifying circulation (left column; difference between the 2140–2160 and the 1990–2010 periods) and weakening circulation (right column; difference between the 2280–2299 and the 2140–2160 periods). Stipplings show regions where the changes are statistically insignificant at the 5% level based on a Student's *t* test.

Fig. 3 | The non-monotonic storm track behavior under abrupt CO_2 forcing. a The North Atlantic eddy kinetic energy (EKE) in the abrupt runs under different CO_2 levels. **b** The response of the eddy growth rate, relative to preindustrial values, to abrupt CO_2 forcing (black line). Also shown are the relative contributions of the zonal wind (red, $\sigma|U$), tropopause height (green, $\sigma|H$), and static stability (blue, $\sigma|N$) to the growth rate response. Error bars show the standard deviation across years from each run.

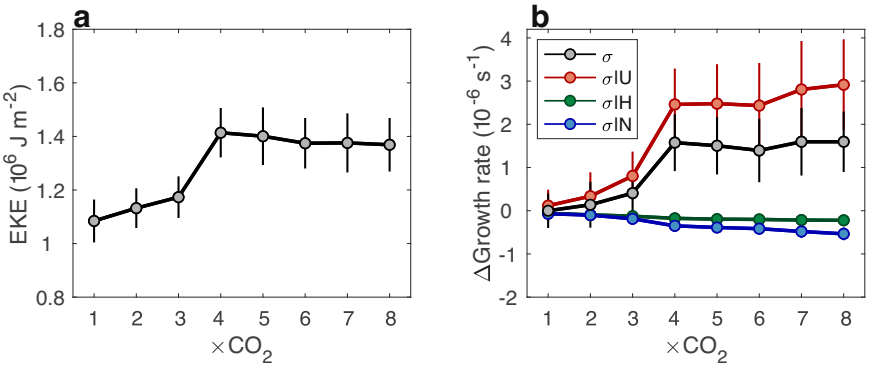

warming to strengthen the mid-latitude storm track, while of polar warming to weaken the storm track[28].

Examining the difference between the warming patterns at low and high CO_2 levels further highlights the importance of the different warming rates in the lower latitudes (Fig. 4c). First, for the same increase in CO_2 concentrations, a weaker warming throughout the troposphere is evident at higher CO_2 levels (blue colors in Fig. 4c). This reduced warming is expected given the logarithmic relationship between CO_2 and surface temperature. Second, although the reduced warming implied by the logarithmic forcing–temperature relationship is evident throughout the troposphere—whose temperature is coupled to that of the surface—it is not spatially uniform. The reduced warming seen in Fig. 4c has a similar pattern, only of an opposite sign, to the canonical atmospheric warming pattern in Fig. 4a. Specifically, the upper tropical troposphere and the lower Arctic troposphere exhibit a larger reduced warming. Similar to the surface warming, which is amplified in the troposphere (Fig. 4a) via internal feedbacks, the reduced warming of the surface (i.e., the logarithmic effect) is also amplified in the atmosphere (e.g., via the moist adiabatic lapse rate in the tropics or the ice-albedo feedback and the associated wintertime oceanic heat release into the lower tropospheric Arctic, that is amplified via the lapse rate feedback[29]). Consistent with previous findings[30], we note that the upper polar troposphere exhibits similar warming at low and high CO_2 levels (Fig. 4c), likely since it is not strongly coupled to the surface warming signal (e.g., unlike the reduced low-level Arctic amplification at high CO_2 levels).

Consequently, most of the difference in the mid-latitude tropospheric warming between low and high CO_2 levels stems from the lower latitudes, where a strong reduced warming is evident throughout the troposphere (Fig. 4c). Indeed, the upper tropical tropospheric warming (averaged

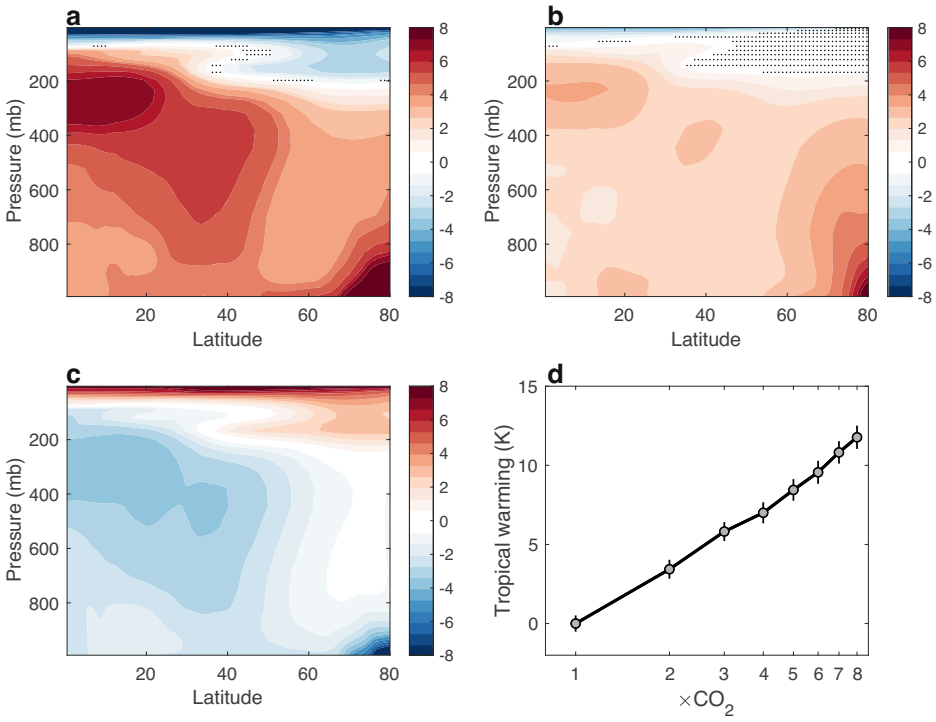

Fig. 4 | The logarithmic CO_2 warming. The response of the North Atlantic atmospheric temperature (K) to an abrupt increase in CO_2 concentrations during (**a**) EKE intensification (between $1 \times CO_2$ and $3 \times CO_2$) and **b** EKE weakening (between $4 \times CO_2$ and $6 \times CO_2$). **c** The difference in the warming at low and high CO_2 concentrations (the difference between panel (**a**) and (**b**)). Stipplings show regions where the changes are statistically insignificant at the 5% level based on a Student's *t* test. **d** The warming of the tropical upper troposphere plotted against CO_2 levels, relative to pre-industrial values; note the linear relation in semilogarithmic axes.

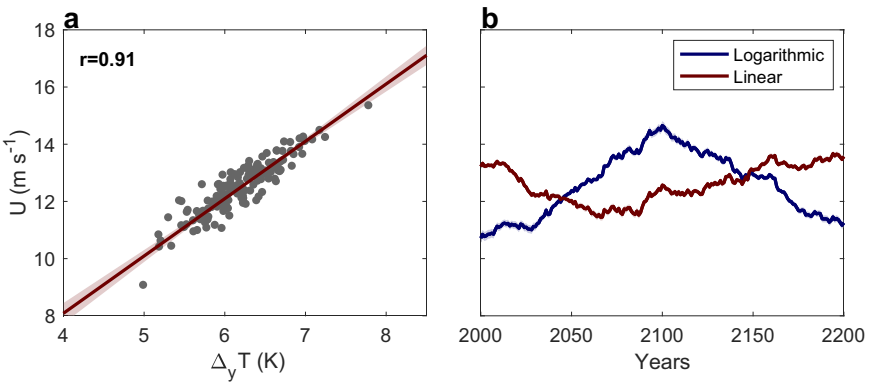

Fig. 5 | The role of logarithmic CO_2 warming in the reversibility of the flow. a The CMIP6 mean jet stream (U) plotted against the meridional temperature gradient ($\Delta_y T$) across different years over the 2000–2200 period (gray dots). Their correlation appears in the upper left corner. Red line and shading show the linear regression ± 2 s.d. ("Methods"). **b** The evolution of the constrained jet stream based on a linear (red) and logarithmic (blue) relation between CO_2 and temperature over the equatorward flank of the jet stream.

between 20° − 40°N at 500 mb) shows a logarithmic relation with CO_2 levels (linear relation in semilogarithmic axes; Fig. 4d). Similar responses are evident in the extended SSP5-8.5 runs, which also show that the warming based on a moist adiabatic lapse rate captures the low latitude warming (Supplementary Fig. 4). We conclude that at low CO_2 levels the upper troposphere at the lower latitudes warms considerably (relative to the higher latitudes), acting to intensify the meridional temperature gradient and the storm track and jet stream. In contrast, at high CO_2 levels, this warming pattern at low latitudes weakens (more than the warming at the higher latitudes), due to the logarithmic relationship between CO_2 and temperature, yielding a reduction in the meridional temperature gradient and the storm track and jet stream intensity, thus explaining the overall non-monotonic behavior of the circulation.

Lastly, we return to the more realistic SSP5-8.5 scenario to further corroborate the role of the logarithmic relation between the tropospheric temperature at the lower latitudes and CO_2 in driving the non-monotonic behavior of the circulation. In particular, we make use of thermal wind balance, which yields a strong linear relationship (r = 0.91) between the meridional temperature gradient ($\Delta_y T$) and the jet stream (U) across different years in the SSP5-8.5 runs (gray dots in Fig. 5a); $\Delta_y T$ is defined as the difference in the zonally averaged North Atlantic temperature at 500 mb between the equatorward (averaged between 40°N − 50°N, T_{low}) and poleward (averaged between 50°N − 60°N, T_{high}) flanks of the jet. Based on the above linear relationship, we next conduct emergent constraint analyses to create two jet stream evolutions: with and without the logarithmic relationship between T_{low} and CO_2.

First, over the 2000–2200 period (when the CO_2 increases), we fit, with respect to CO_2, logarithmic and linear profiles to the temperature over the equatorward flank (T_{low}) (Supplementary Fig. 5). Subtracting from each of these profiles the temperature over the poleward flank (T_{high}) yields two time evolutions of $\Delta_y T$. Second, for each year, we take the $\Delta_y T$ estimated from each profile together with the linear relationship between the meridional temperature gradient and the jet stream, which yields a constrained North Atlantic jet stream ("Methods"). Examining the evolution of the resulting two constrained jet stream profiles reveals that while a logarithmic relationship between T_{low} and CO_2 captures the reversibility of the flow with increasing CO_2 concentrations (blue line Fig. 5b), a linear relationship between T_{low} and CO_2 fails to do so, mostly showing an intensification from the mid-21st century. This analysis demonstrates that the logarithmic relationship between T_{low} and CO_2, and the associated reduced warming

over the lower latitudes (relative to higher latitudes), is key in reversing the meridional temperature gradient changes, and consequently the North Atlantic circulation.

Discussion

The latest report from the Intergovernmental Panel on Climate Change (IPCC), and previous work[31], concluded that there is high confidence in future abrupt and non-monotonic changes in several thermodynamic variables, such as the polar sea- and land-ice and sea-level rise[16]. Since atmospheric flow phenomena are driven by thermodynamic processes, this suggests that the potential for abrupt and non-monotonic changes in the large-scale atmospheric flow should be considered as well. However, to date, changes in the atmospheric flow beyond 2100 have not been thoroughly investigated, further increasing the uncertainty in large-scale flow projections. As a result, mitigation and adaptation strategies, which rely on climate model projections for the 21st century, have not accounted for potential non-monotonic or abrupt flow changes beyond 2100.

Here, we find that under continued CO_2 emissions, the North Atlantic circulation (the jet stream and storm track) intensifies through the mid-22nd century but weakens thereafter, further recovering toward its 20th-century value, by the end of the 23rd century. In addition, this non-monotonic behavior impacts both the North Atlantic Ocean and eastern North America, where the tendency of eddy heat and moisture fluxes to wet and warm the higher mid-latitudes, while drying and cooling the lower mid-latitudes by the mid-22nd century, reverses through the end of the 23rd century.

The non-monotonic behavior of the circulation is shown to result from the logarithmic relationship between CO_2 and temperature. Specifically, the intensification of the circulation is driven by the enhanced warming of the upper troposphere at lower latitudes, relative to higher latitudes[12], which intensifies the meridional temperature gradient and the North Atlantic circulation. As CO_2 concentrations continue to rise, this warming pattern at low latitudes weakens considerably (relative to the higher latitudes) due to the logarithmic relationship between CO_2 and temperature, yielding a weakening of the meridional temperature gradient and of the North Atlantic circulation. We note that since the enhanced warming of the upper troposphere at lower latitudes is strongly coupled to the surface temperature, via the moist diabatic lapse rate, the CO_2 level where the circulation reverses likely depends on the climate sensitivity, as well as on the extension of the upper-level warming pattern into the mid-latitudes.

Our results have two main implications for the timing and design of mitigation pathways. First, the reversibility of the circulation from the mid-22nd century suggests that the coming decades are a critical period for mitigating the impacts of the intensifying North Atlantic circulation. The longer mitigation policies are postponed, the greater the exposure to the impacts of a stronger North Atlantic circulation and the lower the perceived urgency of intervention, owing to the reversibility of the circulation. Second, under the SSP5-8.5 scenario, the CO_2 increases relatively linearly with time over the 22nd century, which yields logarithmic warming with time (and not only with CO_2) and the associated non-monotonicity of the North Atlantic circulation with time. Thus, under a rapid, nonlinear increase in CO_2 emissions, the warming could hinder the reversibility of the circulation with time. We thus stress the importance of limiting the pace of CO_2 increase, as it could impact non-monotonic climate behaviors.

Methods

Climate model simulations

Assessing the North Atlantic circulation response to CO_2 emissions beyond 2100 is conducted by analyzing two sets of climate model simulations. First, we make use of daily and monthly wind, temperature and specific humidity output from model simulations from phase 6 of the Coupled Model Intercomparison Program (CMIP6) under the historical (through 2014) and the Shared Socioeconomic Pathways 5-8.5 (SSP5-8.5) (through 2300)[32]. Specifically, we include all models with available daily output through the 21st, 22nd and 23rd centuries: CanESM5, EC-Earth3-Veg, IPSL-CM6A-LR and MRI-ESM2-0.

Second, given the relatively small amount of models with available daily data (which is necessary for the calculation of the storm track) through 2300, and to cleanly isolate the impact of increased CO_2 concentrations on the non-monotonic behavior of the North Atlantic circulation, we also make use of abrupt CO_2 runs. Specifically, initialized from the preindustrial state, version 1.2 of the Community Earth System Model[33] (CESM) was forced with 2×, 3×, 4×, 5×, 6×, 7×, and 8× the preindustrial CO_2 levels[31]. The last 50 years of each 150-year simulation are used for the analysis.

Circulation indices

To examine the changes in the winter (December–February, DJF) North Atlantic circulation, we analyze two flow variables: the North Atlantic storm track and jet stream. The storm track is defined, following previous studies[10,12,24,34–38], as the vertically integrated eddy kinetic energy (EKE), $\mathrm{EKE} = \frac{1}{g}\int_0^{p_s} u'^2 + v'^2\,dp$, where g is gravity, p_s is surface pressure, u and v are the zonal and meridional winds, respectively, p is pressure and primes denote eddy terms, calculated using a Butterworth bandpass filter of 2.5–6 days. In the CESM runs, due to the lack of daily output across all levels, the eddies are defined as deviations from the monthly mean; nonetheless, they produce similar results[12].

The jet stream is defined as the tropospheric (between 300–1000 mb) averaged zonal wind; the reversibility of the jet stream is apparent throughout the troposphere (Supplementary Fig. 1). To further assess the impacts of the non-monotonic circulation changes, we also examine the eddy (i.e., storm-track induced) heat and moisture flux convergence. The eddy heat and moisture fluxes are defined as the vertically integrated DJF mean $c_p\mathbf{u}'T'$ and $L_v\mathbf{u}'q'$, respectively, where $\mathbf{u}$ is the horizontal wind vector, T and q are the atmospheric temperature and specific humidity, respectively, $c_p = 1004\ \mathrm{J\,kg^{-1}K^{-1}}$ is the specific heat capacity of dry air, and $L_v = 2.5 \times 10^6\ \mathrm{J\,kg^{-1}}$ is the latent heat of vaporization. Lastly, since in the CESM runs the intensification of the circulation does not extend as far westward as in the CMIP6 runs (likely due to the different experimental design, i.e., transient vs. abrupt forcing), we define the North Atlantic region in the abrupt runs between 20°W − 50°E.

Normal mode instability analysis

The eddy growth rate is calculated by applying a linear normal mode instability analysis to the quasigeostrophic equations over the North Atlantic[12,24,36,37,39,40]. Specifically, the linearized (around the North Atlantic mean state) quasigeostrophic equations, with zero vertical velocity at the vertical boundaries, take the following form,

$$\begin{aligned} &\frac{\partial q'}{\partial t} + \bar{\mathbf{u}}\cdot\nabla q' + \mathbf{u}'\cdot\nabla\bar{q} = 0\,, H_p < p < p_s \\ &\frac{\partial}{\partial t}\frac{\partial\psi'}{\partial p} + \bar{\mathbf{u}}\cdot\nabla\frac{\partial\psi'}{\partial p} - \mathbf{u}'\cdot\nabla\frac{\partial\bar{\psi}}{\partial p} = 0,\ p = H_p, p_s, \end{aligned} \tag{1}$$

where overbars and primes denote the North Atlantic mean and deviation therefrom, respectively, ∇ is the horizontal gradient, $q' = \nabla^2\psi' + \Gamma\psi'$ is the eddy quasigeostrophic potential vorticity, $u' = -\frac{\partial\psi'}{\partial y}$ and $v' = \frac{\partial\psi'}{\partial x}$, $\Gamma = \frac{\partial}{\partial p}\frac{f^2}{S^2}\frac{\partial}{\partial p}$, $S^2 = -\frac{1}{\bar{\rho}\bar{\theta}}\frac{\partial\bar{\theta}}{\partial p}$ is static stability, θ is potential temperature, ρ is the density, $\nabla\bar{q} = \Gamma\overline{v}\hat{i} + (\beta - \Gamma\overline{u})\hat{j}$ is the mean quasigeostrophic potential vorticity gradient, β is the meridional derivative of the Coriolis parameter f, and H_p is the tropopause height (defined, following the WMO, as the lowest level where the vertical temperature gradient crosses the 2 K km^{-1} value, and stays, on average, below 2 K km^{-1} in all higher levels within 2 km).

Equation (1) can be written in the form of an eigenvalue problem by assuming that the zonal derivatives of the mean fields (q,ψ) are negligible and substituting a plane-wave solution, $\psi' = \mathrm{Re}\widehat{\psi'}(p)e^{i(kx-\omega t)}$, where k is the zonal wavenumber and ω is the frequency (the eigenvalues). The resulting vertical eigenvalue problem is then solved for each year using the vertically dependent wintertime North Atlantic mean fields (zonal wind,

temperature, tropopause height), and we analyze the resulting fastest growth rate each year. Lastly, to assess the relative contribution of each mean field to the growth rate response, we re-solve the above eigenvalue problem while keeping all mean fields at their preindustrial values (or 1950 values in the transient runs) except for one. In spite of the relative simplicity of the instability analysis, the resulting growth rate adequately captures the EKE behavior (Fig. 3).

Emergent constraint analysis

To date, emergent constraint analyses[41–46] have been mostly used to constrain projected climate changes. By exploiting a linear relation (which is significant and physically robust) across climate models between projected changes and the historical climate, together with observations of the latter, one could refine and confine the range of model projections. Here, we make use of this technique to examine the evolution of the North Atlantic circulation under both a linear and logarithmic relation between CO_2 and the upper tropospheric temperature at the lower mid-latitudes. Specifically, we leverage the strong physical linear relation between the jet stream and the meridional temperature gradient (thermal wind balance). A total least squares linear regression analysis is used to calculate the regression between the CMIP6 mean jet stream and the meridional temperature gradient across different years (over the 2000–2200 period, when the CO_2 increases). The uncertainties in the jet stream and the meridional temperature gradient for the regression analysis are estimated as the standard deviation across years. Bootstrapping the years 100 times with replacement, and repeating the regression analysis for each iteration, yields 100 values of the jet stream for each meridional temperature gradient. The uncertainty in the original regression is then estimated as two standard deviations across the bootstrapped values. We then create two temperature profiles with respect to CO_2 by fitting linear and logarithmic profiles to the temperature over the equatorward flank of the jet stream. By subtracting from these profiles the temperature over the poleward flank of the jet stream at each year, we obtain a time-dependent meridional temperature gradient for each profile. Lastly, using the linear relation between the jet stream and the meridional temperature gradient, together with its uncertainty, we map the artificial meridional temperature gradients to the jet stream and obtain a time-dependent jet stream for both linear and logarithmic CO_2-temperature relationships.

Data availability

The data used in the manuscript are publicly available for CMIP6 (https://esgf-node.llnl.gov/projects/cmip6/), and the CESM data is available upon request.

Received: 23 October 2025; Accepted: 23 December 2025;
Published online: 09 January 2026

References

1. Zappa, G., Shaffrey, L. C., Hodges, K. I., Sansom, P. G. & Stephenson, D. B. A multimodel assessment of future projections of North Atlantic and European extratropical cyclones in the CMIP5 climate models. *J. Clim.* **26**, 5846–5862 (2013).
2. Lehmann, J. & Coumou, D. The influence of mid-latitude storm tracks on hot, cold, dry and wet extremes. *Sci. Rep.* **5**, 17491 (2015).
3. Chang, E. K. M., Ma, C., Zheng, C. & Yau, A. M. W. Observed and projected decrease in Northern Hemisphere extratropical cyclone activity in summer and its impacts on maximum temperature. *Geophys. Res. Lett.* **43**, 2200–2208 (2016).
4. Ionita, M., Nagavciuc, V., Kumar, R. & Rakovec, O. On the curious case of the recent decade, mid-spring precipitation deficit in Central Europe. *npj Clim. Atmos. Sci.* **3**, 49 (2020).
5. Yau, A. M. W. & Chang, E. K. M. Finding storm track activity metrics that are highly correlated with weather impacts. Part I: frameworks for evaluation and accumulated track activity. *J. Clim.* **33**, 10169–10186 (2020).
6. Knight, J. R., Folland, C. K. & Scaife, A. A. Climate impacts of the Atlantic multidecadal oscillation. *Geophys. Res. Lett.* **33**, L17706 (2006).
7. Chang, E. K. M., Guo, Y. & Xia, X. CMIP5 multimodel ensemble projection of storm track change under global warming. *J. Geophys. Res.* **117**, D23118 (2012).
8. Woollings, T., Gregory, J. M., Pinto, J. G., Reyers, M. & Brayshaw, D. J. Response of the North Atlantic storm track to climate change shaped by ocean-atmosphere coupling. *Nat. Geosci.* **5**, 313–317 (2012).
9. Harvey, B. J., Shaffrey, L. C. & Woollings, T. J. Equator-to-pole temperature differences and the extra-tropical storm track responses of the CMIP5 climate models. *Clim. Dyn.* **43**, 1171–1182 (2014).
10. Lehmann, J., Coumou, D., Frieler, K., Eliseev, A. V. & Levermann, A. Future changes in extratropical storm tracks and baroclinicity under climate change. *Env. Res. Lett.* **9**, 084002 (2014).
11. Harvey, B. J., Cook, P., Shaffrey, L. C. & Schiemann, R. The response of the Northern Hemisphere storm tracks and jet streams to climate change in the CMIP3, CMIP5, and CMIP6 climate models. *J. Geophys. Res.* **125**, e32701 (2020).
12. Chemke, R., Zanna, L., Orbe, C., Sentman, L. T. & Polvani, L. M. The future intensification of the North Atlantic winter storm track: the key role of dynamic ocean coupling. *J. Clim.* **35**, 2407–2421 (2022).
13. Liu, W., Fedorov, A. V., Xie, S. & Hu, S. Climate impacts of a weakened Atlantic Meridional overturning circulation in a warming climate. *Sci. Adv.* **6**, eaaz4876 (2020).
14. Seager, R., Naik, N. & Vecchi, G. A. Thermodynamic and dynamic mechanisms for large-scale changes in the hydrological cycle in response to global warming. *J. Clim.* **23**, 4651–4668 (2010).
15. Chang, E. K. M., Yau, A. M. W. & Zhang, R. Finding storm track activity metrics that are highly correlated with weather impacts. Part II: estimating precipitation change associated with projected storm track change over Europe. *J. Clim.* **35**, 2423–2440 (2022).
16. Masson-Delmotte, V. et al. *Climate Change 2021: the Physical Science Basis. Contribution of Working Group I to the Sixth Assessment Report of the Intergovernmental Panel on Climate Change*, 2391 (Cambridge Univ. Press, 2021).
17. O'Gorman, P. A. & Schneider, T. Energy in midlatitude transient eddies in idealized simulations of changed climates. *J. Clim.* **21**, 5797–5806 (2008).
18. Mitevski, I., Chemke, R., Orbe, C. & Polvani, L. M. Southern Hemisphere Winter storm tracks respond differently to low and high CO2 forcings. *J. Clim.* **37**, 5355–5372 (2024).
19. Manzini, E., Karpechko, A. Y. & Kornblueh, L. Nonlinear response of the stratosphere and the North Atlantic-European climate to global warming. *Geophys. Res. Lett.* **45**, 4255–4263 (2018).
20. Zhou, W., Leung, L. R. & Lu, J. Seasonally and regionally dependent shifts of the atmospheric Westerly Jets under global warming. *J. Clim.* **35**, 5433–5447 (2022).
21. Breul, P., Ceppi, P., Simpson, I. R. & Woollings, T. Seasonal and regional jet stream changes and drivers. *Nat. Rev. Earth Environ.* **6**, 824–842 (2025).
22. Yin, J. H. A consistent poleward shift of the storm tracks in simulations of 21st century climate. *Geophys. Res. Lett.* **32**, L18701 (2005).
23. Wu, Y., Ting, M., Seager, R., Huang, H. & Cane, M. A. Changes in storm tracks and energy transports in a warmer climate simulated by the GFDL CM2.1 model. *Clim. Dyn.* **37**, 53–72 (2011).
24. Chemke, R. & Coumou, D. Human influence on the recent weakening of storm tracks in boreal summer. *npj Clim. Atmos. Sci.* **7**, 86 (2024).
25. Butler, A. H., Thompson, D. W. J. & Heikes, R. The steady-state atmospheric circulation response to climate change-like thermal forcings in a simple general circulation model. *J. Clim.* **23**, 3474–3496 (2010).
26. Yuval, J. & Kaspi, Y. Eddy activity sensitivity to changes in the vertical structure of baroclinicity. *J. Atmos. Sci.* **73**, 1709–1726 (2016).

27. Nie, Y., Zhang, Y., Chen, G. & Yang, X. Quantifying Eddy generation and dissipation in the jet response to upper- versus lower-level thermal forcing. *J. Atmos. Sci.* **79**, 2703–2720 (2022).
28. Yuval, J. & Kaspi, Y. Eddy activity response to global warming-like temperature changes. *J. Clim.* **33**, 1381–1404 (2020).
29. Pithan, F. & Mauritsen, T. Arctic amplification dominated by temperature feedbacks in contemporary climate models. *Nat. Geosci.* **7**, 181–184 (2014).
30. Liang, Y. C., Polvani, L. M. & Mitevski, I. Arctic amplification, and its seasonal migration, over a wide range of abrupt CO2 forcing. *npj Clim. Atmos. Sci.* **5**, 14 (2022).
31. Mitevski, I., Orbe, C., Chemke, R., Nazarenko, L. & Polvani, L. M. Non monotonic response of the climate system to abrupt CO2 forcing. *Geophys. Res. Lett.* **48**, e90861 (2021).
32. Eyring, V. et al. Overview of the Coupled Model Intercomparison Project Phase 6 (CMIP6) experimental design and organization. *Geosci. Model Dev.* **9**, 1937–1958 (2016).
33. Hurrell, J. W. et al. The Community Earth System Model: a framework for collaborative research. *Bull. Am. Meteor. Soc.* **94**, 1339–1360 (2013).
34. O'Gorman, P. A. Understanding the varied response of the extratropical storm tracks to climate change. *Proc. Natl. Acad. Sci. USA* **107**, 19176–19180 (2010).
35. Coumou, D., Lehmann, J. & Beckmann, J. The weakening summer circulation in the Northern Hemisphere mid-latitudes. *Science* **348**, 324–327 (2015).
36. Chemke, R. The future poleward shift of Southern Hemisphere summer mid-latitude storm tracks stems from ocean coupling. *Nat. Commun.* **13**, 1730 (2022).
37. Chemke, R., Ming, Y. & Yuval, J. The intensification of winter mid-latitude storm tracks in the Southern Hemisphere. *Nat. Clim. Change* **12**, 553–557 (2022).
38. Chemke, R. Persistent austral winter storm track weakening beyond doubling of CO2 concentrations. *Nat. Commun.* **16**, 1935 (2025).
39. Karbi, I. & Chemke, R. Emergence of winter large-scale transient atmospheric waves in the northern hemisphere. *Geophys. Res. Lett.* **52**, e2024GL113410 (2025).
40. Karbi, I. & Chemke, R. Seasonally asymmetric projected changes in austral atmospheric waves. *Geophys. Res. Lett.* **52**, e2025GL117 (2025).
41. Cox, P. M. et al. Sensitivity of tropical carbon to climate change constrained by carbon dioxide variability. *Nature* **494**, 341–344 (2013).
42. Cox, P. M., Huntingford, C. & Williamson, M. S. Emergent constraint on equilibrium climate sensitivity from global temperature variability. *Nature* **553**, 319–322 (2018).
43. Hall, A., Cox, P., Huntingford, C. & Klein, S. Progressing emergent constraints on future climate change. *Nat. Clim. Change* **9**, 269–278 (2019).
44. Simpson, I. R. et al. Emergent constraints on the large-scale atmospheric circulation and regional hydroclimate: do they still work in CMIP6 and how much can they actually constrain the future? *J. Clim.* **34**, 6355–6377 (2021).
45. Chemke, R. & Yuval, J. Human induced weakening of the Northern Hemisphere tropical circulation. *Nature* **617**, 529–532 (2023).
46. Chemke, R. & Yuval, J. Atmospheric circulation to constrain subtropical precipitation projections. *Nat. Clim. Change* **15**, 287–292 (2025).

Acknowledgements

R.C. is grateful for the support of the Willner Family Leadership Institute for the Weizmann Institute of Science and the Zuckerman STEM Leadership Program. I.M. was supported by a Harry Hess postdoctoral fellowship from Princeton Geosciences. This work is supported by the Israeli Science Foundation Grant 407/25.

Author contributions

R.C. analyzed the data and, together with I.M., discussed and wrote the paper.

Competing interests

The authors declare no competing interests.

Additional information

Supplementary information The online version contains supplementary material available at https://doi.org/10.1038/s41612-025-01314-3.

Correspondence and requests for materials should be addressed to Rei Chemke.